



HAL
open science

Inverse problems in air-saturated porous media via reflected waves

Zine El Abiddine E.A. Fellah, Sébastien Berger, Walter Lauriks, Claude Depollier, Jean-Yves Chapelon

► **To cite this version:**

Zine El Abiddine E.A. Fellah, Sébastien Berger, Walter Lauriks, Claude Depollier, Jean-Yves Chapelon. Inverse problems in air-saturated porous media via reflected waves. *Review of Scientific Instruments*, 2004, 74, pp.2871-2879. 10.1063/1.1569412 . hal-00088277

HAL Id: hal-00088277

<https://hal.science/hal-00088277>

Submitted on 20 Jun 2022

HAL is a multi-disciplinary open access archive for the deposit and dissemination of scientific research documents, whether they are published or not. The documents may come from teaching and research institutions in France or abroad, or from public or private research centers.

L'archive ouverte pluridisciplinaire **HAL**, est destinée au dépôt et à la diffusion de documents scientifiques de niveau recherche, publiés ou non, émanant des établissements d'enseignement et de recherche français ou étrangers, des laboratoires publics ou privés.

Inverse problem in air-saturated porous media via reflected waves

Z. E. A. Fellah^{a)}

INSERM, unité 556, 151 cours Albert Thomas, 69424 Lyon cedex 03, France

S. Berger and W. Lauriks

Laboratorium voor Akoestiek en Thermische Fysica, Katholieke Universiteit Leuven, Celestijnenlaan 200 D, B-3001 Heverlee, Belgium

C. Depollier

Laboratoire d'Acoustique de l'Université du Maine, UMR-CNRS 6613, Université du Maine, Avenue Olivier Messiaen 72085 Le Mans cedex 09, France

J. Y. Chapelon

INSERM, unité 556, 151 cours Albert Thomas, 69424 Lyon cedex 03, France

Direct and inverse scattering problem in air filled porous materials is solved. A simple ultrasonic reflectivity method is proposed for measuring the porosity of porous materials having a rigid frame. The proposed method is based on a temporal model of the direct and inverse scattering problem for the propagation of transient ultrasonic waves in a homogeneous isotropic slab of porous material having a rigid frame. This time domain model of wave propagation was initially introduced by the authors [Z. E. A. Fellah and C. Depollier, *J. Acoust. Soc. Am.* **107**, 683 (2000)]. The viscous and thermal losses of the medium are described by the model devised by Johnson *et al.* [D. L. Johnson, J. Koplik, and R. Dashen, *J. Fluid. Mech.* **176**, 379 (1987)] and J. F. Allard (Chapman and Hall, London, 1993)] modified by a fractional calculus-based method applied in the time domain. The reflected acoustic wave by air filled porous media can be approximated by the reflected wave at the first interface. The expression of the reflection coefficient is reduced to a simple expression depending on porosity, tortuosity, and incidence angle. An expression of the porosity function of the tortuosity and incidence angle is obtained by solving the inverse problem. Experimental and numerical validation results of this method are presented. This method has the advantage of being rapid and efficient.

I. INTRODUCTION

Porous media filled with air, such as fibrous mats, plastic foams, and various felts, are heavily used in the automotive, aeronautical, and building industries to attenuate sound waves. In the recent past, low-frequency (i.e., in the range 20–600 kHz) ultrasonic techniques have amply proven to be a powerful tool to probe the acoustical properties of these materials. The determination of the properties of a medium using waves that have been reflected by or transmitted through the medium is a classical inverse scattering problem. Such problems are often approached by taking a physical model of the scattering process, generating a synthetic response for a number of assumed values for the parameters, and adjusting these parameters until a reasonable level of correspondence is attained between the synthetic response and the data observed.

One important parameter which appears in theories of sound propagation in porous materials^{1–13} is porosity. Porosity is the relative fraction, by volume, of the air contained within the material. Unlike other parameters included in the description of different various phenomena occurring in the acoustical propagation of porous media at high-frequency

range such as tortuosity,¹¹ viscous characteristic length,⁵ and thermal characteristic length,¹² or at low-frequency range such as flow resistivity¹¹ and thermal permeability,¹³ porosity is a key parameter that plays an important role in propagation at all frequencies. As such, in studies of acoustical properties of porous materials, it is extremely useful to be able to measure this parameter.

Beranek¹⁰ described an apparatus (porosimeter) used to measure the porosity of porous materials. This device was based on the equation of state for ideal gases at a constant temperature (i.e., Boyle's law). Porosity can be determined by measuring the change in air pressure occurring with a known change in volume of the chamber containing the sample. In the Beranek apparatus, both pressure and volume changes are monitored using a U-shaped fluid-filled manometer. An alternate technique for measuring porosity is a dynamic method proposed by Leonard.¹⁴ Techniques that use water as the pore-filling fluid, rather than air, are common in geophysical studies.^{15,16} Mercury has been used as the pore-filling fluid in other applications.¹⁷ However, for many materials, the introduction of liquids into the material is not appropriate. Recently, a similar device to that of Beranek's, involving the use of an electronic pressure transducer, was introduced by Champoux *et al.*¹⁸ This device can be used to

^{a)}Electronic mail: fellah@lyon.inserm.fr

accurately measure very slight changes in pressure, and the output can be recorded by a computer.

In this work, the inverse problem in porous material having a rigid frame is solved using reflected waves data and a simple ultrasonic method of measuring porosity by measuring a wave reflected by a slab of porous material is presented. This method is based on a temporal model of the direct and inverse scattering problem for the propagation of transient ultrasonic waves in a homogeneous isotropic slab of porous material having a rigid frame. This work was initially introduced by the authors of Refs. 1–4. The viscous and thermal losses of the medium are described by the Johnson *et al.*⁵ and Allard⁶ model modified by a fractional calculus-based method in order to be used in the time domain. Reflection and transmission scattering operators of a slab of porous material are derived at oblique incidence and thus the responses of the medium to an incident acoustic pulse are obtained.

The outline of this work is as follows. In Sec. II, a time domain model is given, the connection between the fractional derivatives and wave propagation in rigid porous media in the high-frequency range is established and the basic equations are written in the time domain. Section III is devoted to the direct problem and to the expressions of the reflection and transmission kernels in the time domain and numerical results are given. Section IV deals with the inverse problem and an expression of porosity based on the incident and reflected waves from a slab of porous materials is established. Finally, in Sec. V, the experimental results are given to validate this method.

II. MODEL

In the acoustics of porous materials, a distinction can be made between two situations depending on whether or not the frame is moving. In the first case, the dynamics of the waves due to the coupling between the solid frame and the fluid are clearly described by the Biot theory.^{7,8} In air-saturated porous media, the structure is generally motionless and the waves propagate only in the fluid. This case is described by the model of equivalent fluid which is a particular case in the Biot model, in which the interactions between the fluid and the structure are taken into account in two frequency response factors: The dynamic tortuosity of the medium $\alpha(\omega)$ given by Johnson *et al.*⁵ and the dynamic compressibility of the air included in the porous material $\beta(\omega)$ given by Allard.⁶ In the frequency domain, these factors multiply the density of the fluid and its compressibility, respectively, and represent the deviation from the behavior of the fluid in free space as the frequency increases. In the time domain, they act as operators, and in the high-frequency approximation their expressions are given by Fella and Depollier^{1,2} and Fella, Depollier, and Fella^{3,4} as

$$\bar{\alpha}(t) = \alpha_\infty \left(\delta(t) + \frac{2}{\Lambda} \left(\frac{\eta}{\pi \rho_f} \right)^{1/2} t^{-1/2} \right), \quad (1)$$

$$\bar{\beta}(t) = \left(\delta(t) + \frac{2(\gamma-1)}{\Lambda'} \left(\frac{\eta}{\pi Pr \rho_f} \right)^{1/2} t^{-1/2} \right). \quad (2)$$

In Eqs. (1) and (2), $\delta(t)$ is the Dirac function, Pr is the Prandtl number, η and ρ_f are the fluid viscosity and the fluid density, respectively, and γ is the adiabatic constant. The relevant physical parameters of the model are the tortuosity of the medium α_∞ initially introduced by Zwikker and Kosten¹¹ and the viscous and the thermal characteristic lengths Λ and Λ' introduced by Johnson *et al.*⁵ and Allard.⁶ In this model, the time convolution of $t^{-1/2}$ with a function is interpreted as a semiderivative operator following the definition of the fractional derivative of order ν given in Samko *et al.*,¹⁹

$$D^\nu[x(t)] = \frac{1}{\Gamma(-\nu)} \int_0^t (t-u)^{-\nu-1} x(u) du, \quad (3)$$

where $\Gamma(x)$ is the gamma function.

In this framework, the basic equations of our model can be expressed as

$$\rho_f \bar{\alpha}(t) * \frac{\partial v_i}{\partial t} = -\nabla_i p$$

and

$$\frac{\bar{\beta}(t)}{K_a} * \frac{\partial p}{\partial t} = -\nabla \cdot v, \quad (4)$$

where $*$ denotes the time convolution operation, p is the acoustic pressure, v is the particle velocity and K_a is the bulk modulus of the air. The first equation is the Euler equation, and the second is a constitutive equation obtained from the equation of mass conservation associated with the behavior (or adiabatic) equation.

For a wave propagating at oblique incidence in the plan (xoz) and making an angle θ along the x axis, these equations become:

$$\begin{aligned} \rho_f \alpha_\infty \frac{\partial v_x(x,z,t)}{\partial t} + \frac{2\rho_f \alpha_\infty}{\Lambda} \left(\frac{\eta}{\pi \rho_f} \right)^{1/2} \int_0^t \frac{\partial v(x,z,t)/dt'}{\sqrt{t-t'}} dt' \\ = -\frac{\partial p(x,z,t)}{\partial x}, \\ \rho_f \alpha_\infty \frac{\partial v_x(x,z,t)}{\partial t} + \frac{2\rho_f \alpha_\infty}{\Lambda} \left(\frac{\eta}{\pi \rho_f} \right)^{1/2} \int_0^t \frac{\partial v(x,z,t)/dt'}{\sqrt{t-t'}} dt' \\ = -\frac{\partial p(x,z,t)}{\partial z}, \\ \frac{1}{K_a} \frac{\partial p(x,z,t)}{\partial t} + \frac{2(\gamma-1)}{K_a \Lambda'} \left(\frac{\eta}{\pi \rho_f P_r} \right)^{1/2} \int_0^t \frac{\partial p(x,z,t)/dt'}{\sqrt{t-t'}} dt' \\ = -\frac{\partial v(x,z,t)}{\partial x} - \frac{\partial v(x,z,t)}{\partial z}, \end{aligned} \quad (5)$$

where v_x , v_z are the components of the particle velocity along the axis ox and oz .

In Eq. (5), the convolutions express the dispersive nature of the porous material. They take into account the memory effects due to the fact that the response of the medium to the wave excitation is not instantaneous but needs more time to take effect. The retarding force is no longer proportional to

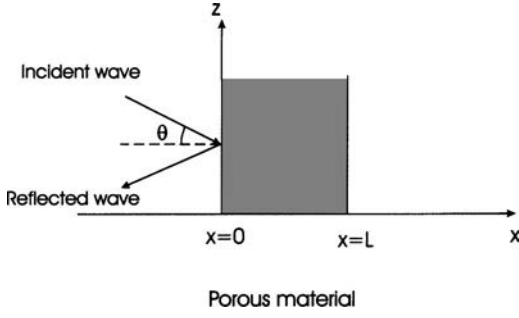


FIG. 1. Geometry of the problem.

the time derivative of the acoustic velocity but is found to be proportional to the fractional derivative of order $1/2$ of this quantity. This occurs because the volume of fluid involved in the motion is not throughout the whole length of the signal as it is in the case of a fully developed steady flow. The phenomenon may be understood by considering such a volume of fluid in a pore to be in harmonic motion. At high frequencies, only a thin layer of fluid is excited and so the average shear stress is high. At a lower frequency, the same amplitude of fluid motion allows a thicker layer of fluid to participate in the motion and, consequently, the shear stress is lower. The penetration distance of the viscous forces and, therefore, the excitation of the fluid depends on frequency. In the time domain, such a dependence is associated with a fractional derivative.

III. DIRECT PROBLEM

The direct scattering problem is that of determining the scattered field, as well as the internal field, that arises when a known incident field impinges on the porous material with known physical properties. To compute the solution of the direct problem, it is necessary to know the reflection and/or the transmission scattering operators which depends on the Green³ function of the porous medium. In that case, the reflected field is given by the convolution of the reflection operator with the incident field, and the transmitted field is given by the convolution of the transmission operator by the incident field.

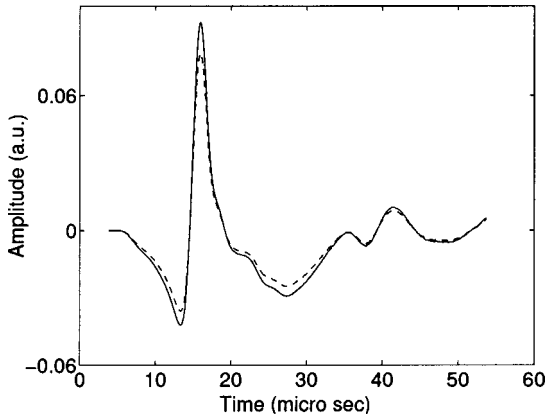


FIG. 2. Transmitted simulated signals for $\phi=0.98$ (solid line) and for $\phi=0.49$ (dashed line).

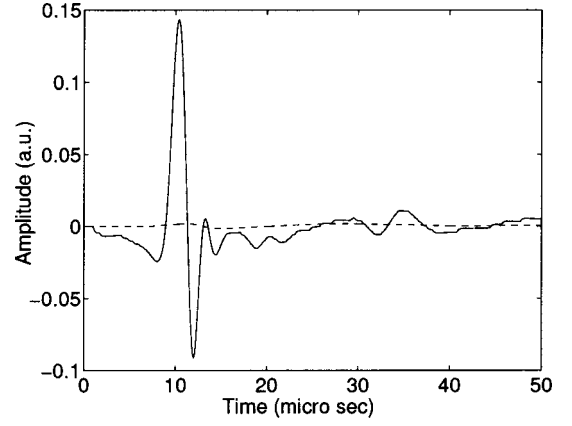


FIG. 3. Numerical simulations of the reflections contributions at the first interface (solid line) and second interface (dashed line).

Consider a homogeneous slab of porous material which occupies the region $0 \leq x \leq L$. The geometry of the problem is shown in Fig. 1. This medium is assumed to be isotropic and to have a rigid frame. A short sound pulse impinges at oblique incidence on the medium from the left-hand side. It gives rise to an acoustic pressure field $p(x,t)$ and an acoustic velocity field $v(x,t)$ within the material, which satisfies the propagation equation¹⁻⁴

$$\frac{\partial^2 p(x,z,t)}{\partial x^2} - A \frac{\partial^2 p(x,z,t)}{\partial t^2} - B \frac{\partial^{3/2} p(x,z,t)}{\partial t^{3/2}} - C \frac{\partial p(x,z,t)}{\partial t} = 0, \quad (6)$$

where the coefficients A , B , and C are constants, respectively, given by

$$A = \frac{1}{c_0^2} (\alpha_\infty - \sin^2 \theta), \quad B = \frac{2\alpha_\infty}{K_a} \sqrt{\frac{\rho_f \eta}{\pi}} \times \left(\frac{1}{\Lambda} + \frac{\gamma-1}{\sqrt{Pr\Lambda'}} \right), \quad C = \frac{4\alpha_\infty(\gamma-1)\eta}{K_a \Lambda \Lambda' \sqrt{Pr}}. \quad (7)$$

The first one is related to the velocity of the projected wave along the x axis $c = c_0 / \sqrt{\alpha_\infty - \sin^2 \theta}$. The other coefficients are essentially dependent of the characteristic lengths Λ and

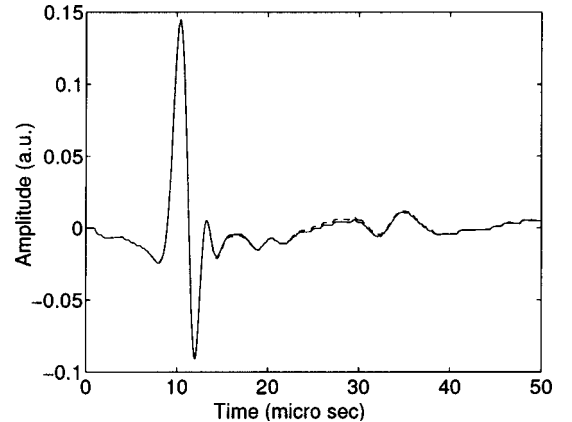


FIG. 4. Reflected wave at the interface $x=0$ (solid line) and the total reflected wave (dashed line).

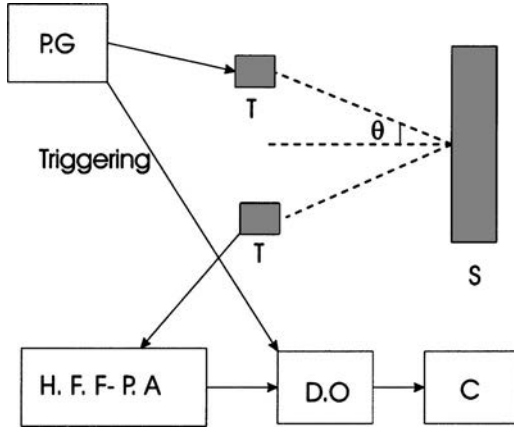


FIG. 5. Experimental setup of the ultrasonic measurements in reflected mode. PG: pulse generator; HFF-PA: high-frequency filtering-preamplifier; DO: digital oscilloscope; C: computer; T: transducer; and S: sample.

Λ' and express the viscous and thermal interactions between the fluid and the structure. The constant B governs the spreading of the signal while C is responsible for the attenuation of the wave. Obviously, a knowledge of these three coefficients allows the determination of the parameters α_∞ , Λ , and Λ' . One way to solve Eq. (7) with suitable initial and boundary conditions is by using the Laplace transform. The approach is quite simple although the inverse Laplace transform requires tedious calculus.³ A suitable setting for the

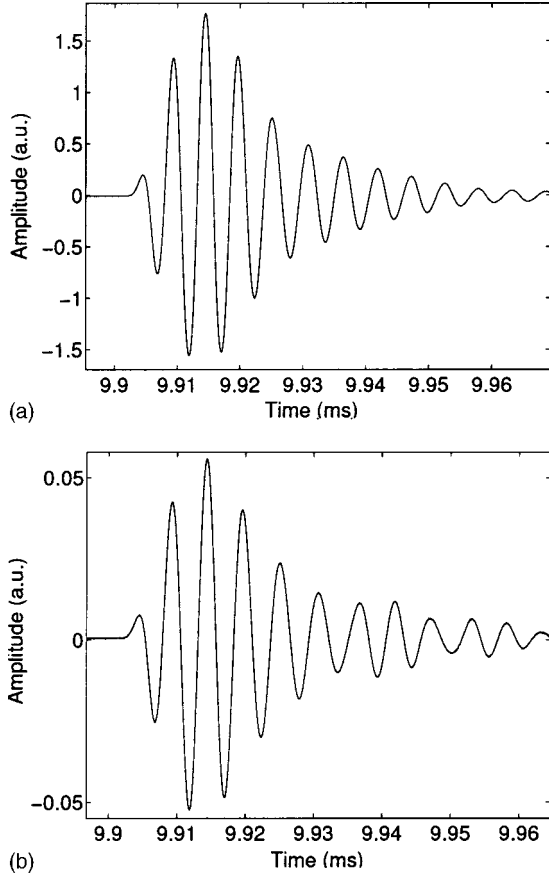


FIG. 6. (a) Experimental incident signal ($\theta=17^\circ$). (b) Experimental reflected signal by the plastic foam M2 ($\theta=17^\circ$).

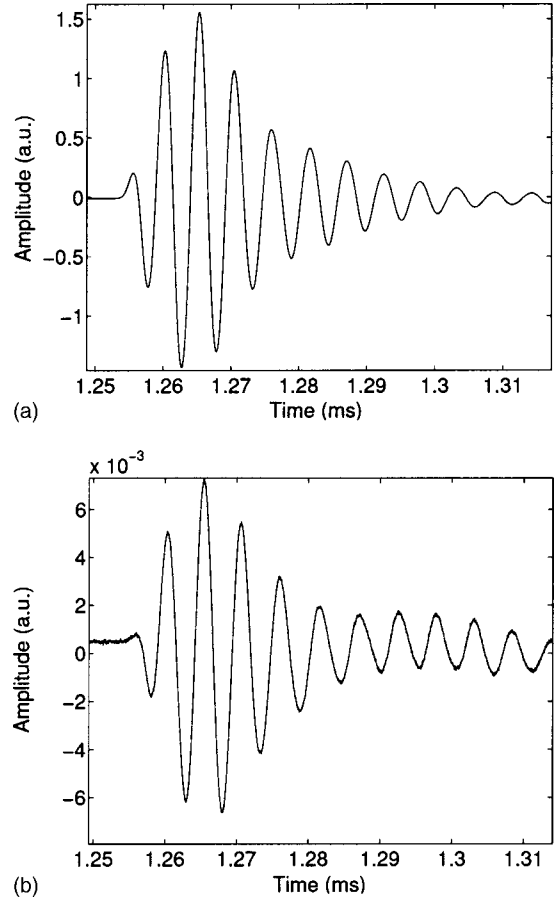


FIG. 7. (a) Experimental incident signal ($\theta=53^\circ$). (b) Experimental reflected signal by the plastic foam M2 ($\theta=53^\circ$).

introduction of the time domain solution of the modified wave propagation [Eq. (6)] is provided by the following model.

To derive the reflection and transmission scattering operators, it is assumed that the pressure field and the flow velocity are continuous at the boundary of the material

$$p(0^+, t) = p(0^-, t), \quad p(L^-, t) = p(L^+, t), \quad (8)$$

$$v(0^-, t) = \phi v(0^+, t), \quad v(L^+, t) = \phi v(L^-, t),$$

where ϕ is the porosity of the medium and \pm superscripts denotes the limit from the left- and the right-hand side, respectively. The initials conditions are given by

$$p(x, t)|_{t=0} = 0, \quad \left. \frac{\partial p}{\partial t} \right|_{t=0} = 0, \quad (9)$$

which means that the medium is idle for $t=0$.

If the incident sound wave is launched in the region $x \leq 0$, then the general solution of Eq. (6) in the region to the left-hand side of the material is the sum of the incident and reflected field

$$p_1(x, t) = p^i \left(t - \frac{x \cos \theta}{c_0} \right) + p^r \left(t + \frac{x \cos \theta}{c_0} \right), \quad x < 0. \quad (10)$$

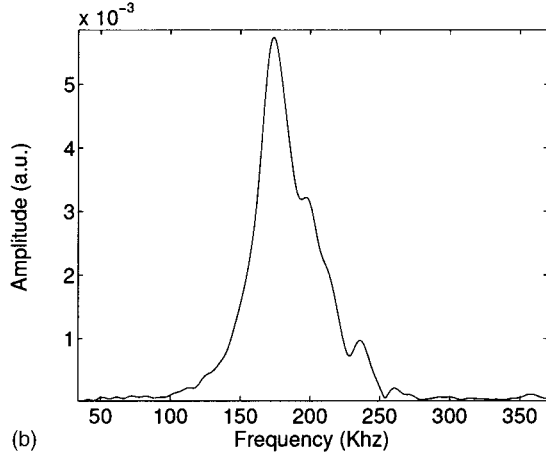
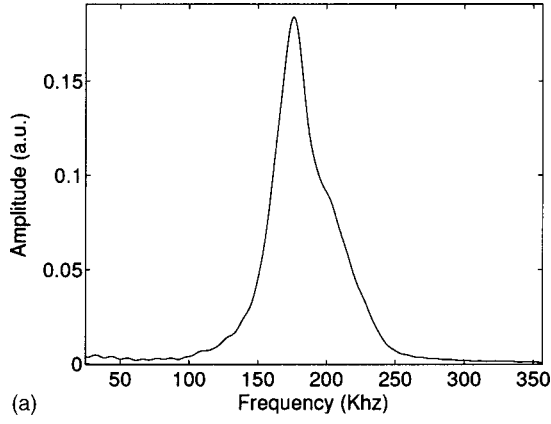


FIG. 8. (a) Spectrum of the incident signal ($\theta=17^\circ$). (b) Spectrum of the reflected signal ($\theta=17^\circ$).

Here, $p_1(x,t)$ is the field in the region $x < 0$, p^i and p^r denote the incident and the reflected field, respectively. In addition, a transmitted field is produced in the region to the right-hand side of the material. This has the form

$$p_3(x,t) = p^t \left(t - \frac{L}{c} - \frac{(x-L)\cos\theta}{c_0} \right), \quad x > L, \quad (11)$$

where $p_3(x,t)$ is the field in the region $x > L$ and p^t is the transmitted field.

The incident and scattered fields are related by the scattering operators (i.e., reflection and transmission operators) for the material. These are integral operators represented by

$$\begin{aligned} p^r(x,t) &= \int_0^t \tilde{R}(\tau) p^i \left(t - \tau + \frac{x}{c_0} \right) d\tau \\ &= \tilde{R}(t) * p^i(t) * \delta \left(t + \frac{x \cos \theta}{c_0} \right), \end{aligned} \quad (12)$$

$$\begin{aligned} p^t(x,t) &= \int_0^t \tilde{T}(\tau) p^i \left(t - \tau - \frac{L}{c} - \frac{(x-L)}{c_0} \right) d\tau \\ &= \tilde{T}(t) * p^i(t) * \delta \left(t - \frac{L}{c} - \frac{(x-L)\cos\theta}{c_0} \right). \end{aligned} \quad (13)$$

In Eqs. (12) and (13), the functions \tilde{R} and \tilde{T} are the reflection and the transmission kernels, respectively, for incidence of waves from the left-hand side. Note that the lower

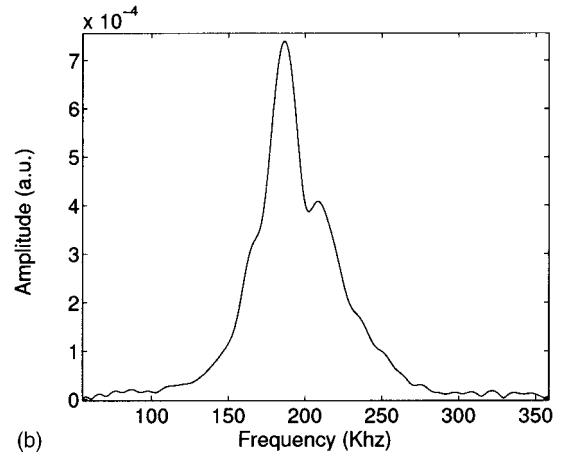
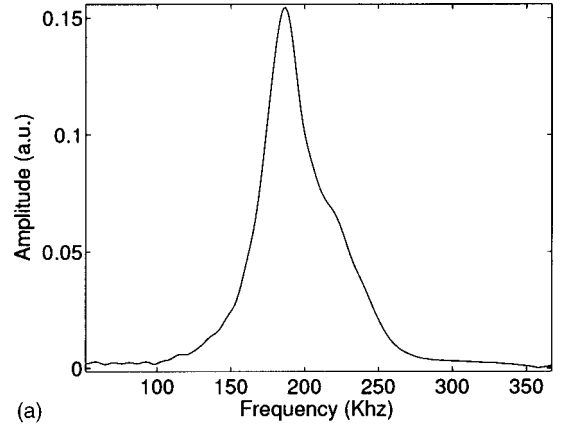


FIG. 9. (a) Spectrum of the incident signal ($\theta=53^\circ$). (b) Spectrum of the reflected signal ($\theta=53^\circ$).

limit of integration in Eqs. (12) and (13) is set to 0, which is equivalent to assuming that the incident wave front first impinges on the material at $t=0$. The scattering operators given in Eqs. (12) and (13) are independent of the incident field used in the scattering experiment and depend only on the properties of the materials. Using Eqs. (4), (6), (8), (12), and (13) and Laplace transform calculus, we can derive the reflection and transmission scattering operators given by

$$\begin{aligned} \tilde{R}(t) &= \left(\frac{\alpha_\infty \cos \theta - \phi \sqrt{\alpha_\infty - \sin^2 \theta}}{\alpha_\infty \cos \theta + \phi \sqrt{\alpha_\infty - \sin^2 \theta}} \right) \\ &\times \sum_{n \geq 0} \left(\frac{\alpha_\infty \cos \theta - \phi \sqrt{\alpha_\infty - \sin^2 \theta}}{\alpha_\infty \cos \theta + \phi \sqrt{\alpha_\infty - \sin^2 \theta}} \right)^{2n} \\ &\times \left[F \left(t, 2n \frac{L}{c} \right) - F \left(t, (2n+2) \frac{L}{c} \right) \right], \end{aligned} \quad (14)$$

TABLE I. Optimized values of the porosity calculated by solving the inverse problem for the plastic foam M2.

Incidence angle θ (degrees)	0	17	23	35	53.5
Porosity ϕ	0.969	0.969	0.971	0.973	0.969

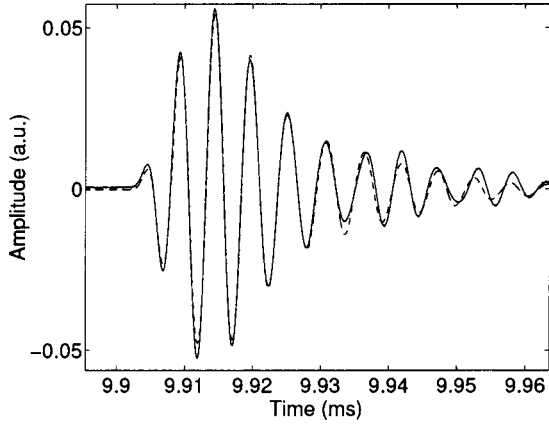


FIG. 10. Comparison between experimental reflected signal (solid line) and simulated reflected signal (dashed line) for M2 ($\theta=17^\circ$).

$$\begin{aligned} \tilde{T}(t) = & \frac{4\phi \cos \theta \sqrt{\alpha_\infty - \sin^2 \theta}}{\left(\sqrt{\alpha_\infty} \cos \theta + \phi \sqrt{1 - \frac{\sin^2 \theta}{\alpha_\infty}} \right)^2} \\ & \times \sum_{n \geq 0} \left(\frac{\alpha_\infty \cos \theta - \phi \sqrt{\alpha_\infty - \sin^2 \theta}}{\alpha_\infty \cos \theta + \phi \sqrt{\alpha_\infty - \sin^2 \theta}} \right)^{2n} \\ & \times F\left(t + \frac{L}{c_0}, (2n+1) \frac{L}{c}\right). \end{aligned} \quad (15)$$

These expressions takes into account the n -multiple reflections in the material. For a positive constant k , $F(t, k)$ is the Green function of the porous material given in Ref. 3 (Appendix).

In most cases, for porous materials saturated by air, the multiple reflection effects are negligible because of the high attenuation of sound waves in this kind of media. So, by taking into account only the reflections at the interfaces $x=0$ and $x=L$, the kernel of transmission is given by

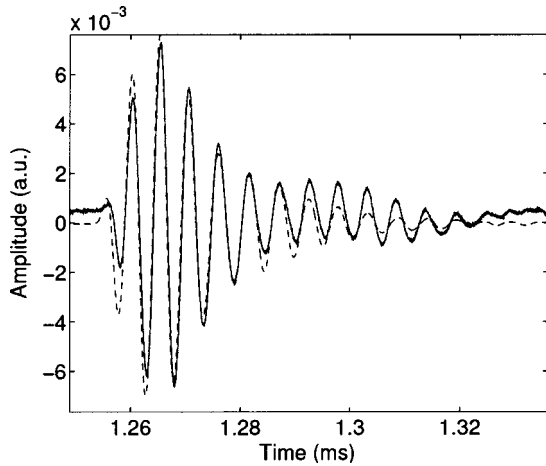


FIG. 11. Comparison between experimental reflected signal (solid line) and simulated reflected signal (dashed line) for M2 ($\theta=53^\circ$).

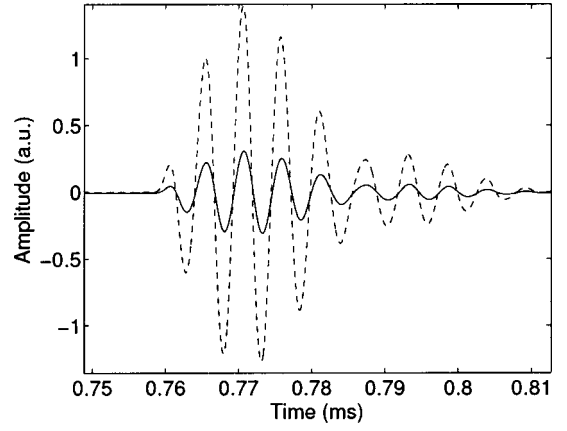


FIG. 12. Experimental incident signal (dashed line) and experimental reflected signal (solid line) by the material M3 for $\theta=13^\circ$.

$$\tilde{T}(t) = \frac{4\phi \cos \theta \sqrt{\alpha_\infty - \sin^2 \theta}}{\left(\sqrt{\alpha_\infty} \cos \theta + \phi \sqrt{1 - \frac{\sin^2 \theta}{\alpha_\infty}} \right)^2} F\left(t + \frac{L}{c}, \frac{L}{c}\right), \quad (16)$$

and the kernel of reflection by

$$\tilde{R}(t) = r(t) + \mathfrak{R}(t), \quad (17)$$

with

$$r(t) = \left(\frac{\alpha_\infty \cos \theta - \phi \sqrt{\alpha_\infty - \sin^2 \theta}}{\alpha_\infty \cos \theta + \phi \sqrt{\alpha_\infty - \sin^2 \theta}} \right) \quad (18)$$

and

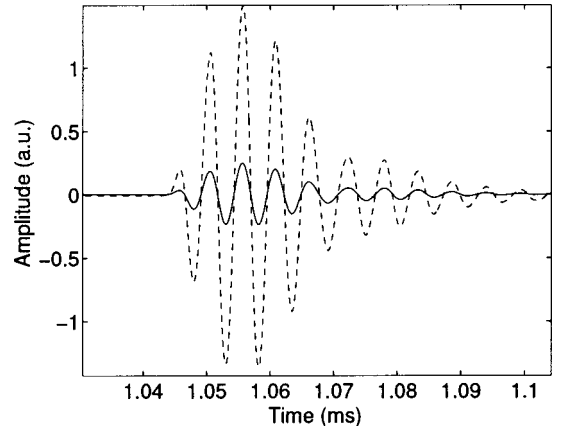


FIG. 13. Experimental incident signal (dashed line) and experimental reflected signal (solid line) by the material M3 for $\theta=39^\circ$.

$$\mathfrak{R}(t) = - \frac{4\phi \cos \theta \sqrt{\alpha_\infty - \sin^2 \theta} \left(\sqrt{\alpha_\infty} \cos \theta - \phi \sqrt{1 - \frac{\sin^2 \theta}{\alpha_\infty}} \right)}{\left(\sqrt{\alpha_\infty} \cos \theta + \phi \sqrt{1 - \frac{\sin^2 \theta}{\alpha_\infty}} \right)} F\left(t, \frac{2L}{c}\right), \quad (19)$$

in the case of a semi-infinite medium when $L \rightarrow \infty$; $F(t, 2L/c) \rightarrow 0$, and $\tilde{R}(t) \rightarrow r(t)$ (Appendix). This means that $r(t)$ is equivalent to the reflection at the interface $x=0$ and that $\mathfrak{R}(t)$ is equivalent to reflection at the interface $x=L$, which is the bulk contribution to the reflection. The part of the wave corresponding to $r(t)$ is not subjected to the dispersion but it is simply multiplied by the factor $(\alpha_\infty \cos \theta - \phi \sqrt{\alpha_\infty - \sin^2 \theta}) / (\alpha_\infty \cos \theta + \phi \sqrt{\alpha_\infty - \sin^2 \theta})$. This shows that although tortuosity is a bulk parameter, it may be evaluated from the wave reflected at the first interface when the porosity is known and vice versa. Although generally speaking, it is easy to evaluate the tortuosity from transmitted waves,^{3,4,20,21} this is not the case for porosity because of its weak sensitivity in transmitted mode. Figure 2 shows two simulated transmitted signals for a plastic foam M1, the first one (solid line) corresponds to the value of porosity $\phi_1 = 0.98$ and the second one (dashed line) corresponds to $\phi_2 = 0.49$. The parameters of the plastic foam M1 (thickness 1.1 cm, $\alpha_\infty = 1.25$, $\Lambda = 50 \mu\text{m}$, and $\Lambda' = 150 \mu\text{m}$) have been determined using conventional methods.^{3,4,20,21} Readers can see the slight difference between the two curves for a 50% difference in porosity values, which is due to the dispersion phenomenon that is governed by viscous, thermal, and inertial effects contributed by α_∞ , Λ and Λ' , and plays a more important role in the Green function $F(t, k)$ than ϕ .

Figure 3 shows the two contributions to the reflection: $r(t)$ (solid line) and $\mathfrak{R}(t)$ (dashed line) for a plastic foam M1 at normal incidence ($\theta=0$). The contribution of $\mathfrak{R}(t)$ to the reflection is negligible when it is compared to the contribution of $r(t)$. In Fig. 4 we show, by numerical simulation, the difference between the reflected wave at the first interface and the total reflected wave. The difference between the two curves is slight. This means that the wave reflected by the

slab may be approximated by the reflected wave by the first interface $r(t)$ with a good level of accuracy. It is easy to verify that this approximation is valid for any incidence angle θ . In Sec. IV, we will show by solving the inverse problem how it is possible to measure the porosity by measuring the reflected wave by a slab of porous material.

IV. INVERSE PROBLEM

A porous material having a rigid frame is characterized by four parameters in the high-frequency range, namely, porosity ϕ , tortuosity α_∞ , the viscous characteristic length Λ , and the thermal characteristic length Λ' . These values are crucial for the behavior of the sound waves in such materials. So, it is therefore fairly important to work out new experimental methods and efficient tools to assess them. Therefore, a basic inverse problem associated with the slab may be stated as follows: To find the values of the parameters of the medium from the measurements of the transmitted and/or reflected signals outside the slab. As shown in Sec. III, the solution to the direct problem is the system of two operators expressed as functions on ϕ , α_∞ , Λ , and Λ' . The inversion algorithm for finding the values of the parameters of the slab is based on a fitting procedure. To find the values of the parameters ϕ , α_∞ , Λ , and Λ' such that the transmitted and reflected signal describes the scattering problem in the best possible way (e.g., in the least-squares sense). Solving the inverse problem using experimental data from transmitted waves is treated^{3,4} and an estimation of α_∞ , Λ , and Λ' has been given with a good level of correspondence from ultrasonic measurements. Here, we will try to solve the inverse problem using experimental reflected wave data for different

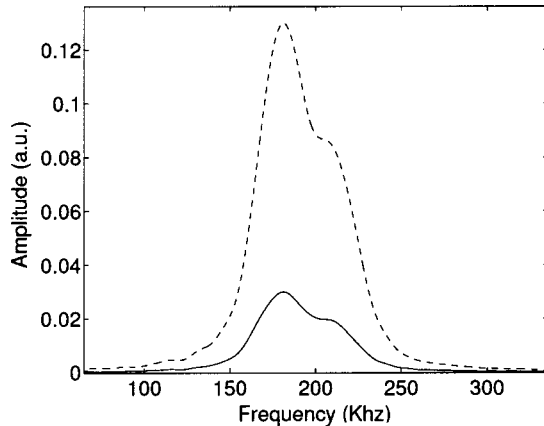


FIG. 14. Spectrum of experimental incident signal (dashed line) and spectrum of experimental reflected signal (solid line) for $\theta = 13^\circ$.

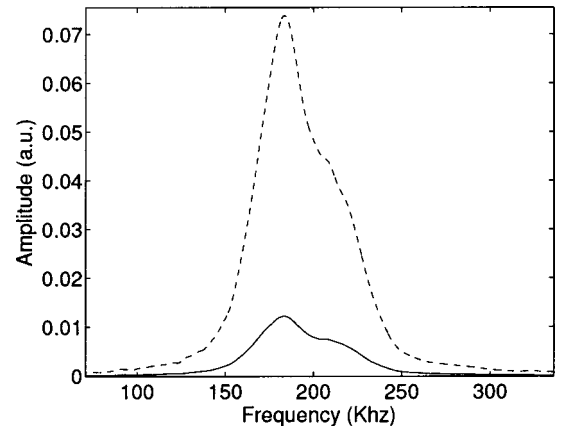


FIG. 15. Spectrum of experimental incident signal (dashed line) and spectrum of experimental reflected signal (solid line) for $\theta = 39^\circ$.

TABLE II. Optimized values of the porosity calculated by solving the inverse problem for the plastic foam M3.

Incidence angle θ (degrees)	0	13	23	39	49
Porosity ϕ	0.820	0.821	0.820	0.821	0.821

values of the incidence angle θ , with the aim of returning to the porosity which, because of its weak sensitivity, cannot be characterized in transmitted mode.

The inverse problem is to find the porosity value ϕ which minimizes the function

$$U = \sum_{i=1}^{i=N} (p^r(t_i) - p_{\text{exp}}^r(t_i))^2, \quad (20)$$

where $p^r(t_i)_{i=1,2,\dots,N}$ represents the discrete set of values of the simulated reflected signal given by Eq. (12) and $p_{\text{exp}}^r(t_i)_{i=1,2,\dots,N}$ is the discrete set of values of the experimental signal. In the approximation that the reflected wave is essentially due to the reflection at the first interface $x=0$;

$$\tilde{R}(t) = r(t) = \frac{a-1}{a+1} \delta(t), \quad (21)$$

where

$$a = \frac{\alpha_{\infty} \cos \theta}{\phi \sqrt{\alpha_{\infty} - \sin^2 \theta}} \quad (22)$$

and

$$p^r(t_i) = \frac{a-1}{a+1} p^i(t_i), \quad (23)$$

where $p^i(t_i)$ is the discrete set of values of the experimental incident signal given out by the transducer. To minimize $U(a)$, we must have

$$\frac{\partial U}{\partial a} = 0 \quad \text{and} \quad \frac{\partial^2 U}{\partial a^2} > 0, \quad (24)$$

$$\frac{\partial U}{\partial a} = \frac{\partial}{\partial a} \sum_{i=1}^{i=N} \left(\frac{a-1}{a+1} p^i(t_i) - p_{\text{exp}}^r(t_i) \right)^2 = 0, \quad (25)$$

then

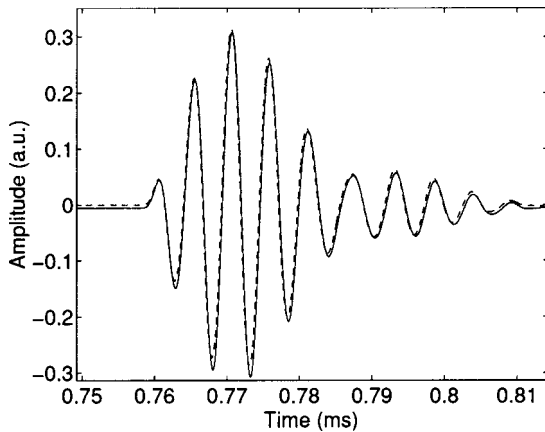


FIG. 16. Comparison between experimental reflected signal (solid line) and simulated reflected signal (dashed line) for M3 ($\theta=13^\circ$).

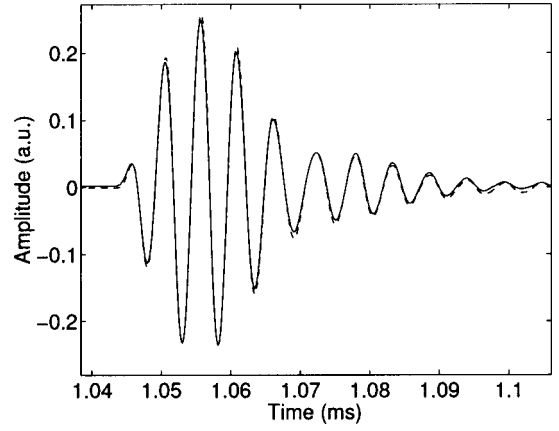


FIG. 17. Comparison between experimental reflected signal (solid line) and simulated reflected signal (dashed line) for M3 ($\theta=39^\circ$).

$$2 \sum_{i=1}^{i=N} \frac{(a+1) - (a-1)}{(a+1)^2} p^i(t_i) \left(\frac{a-1}{a+1} p^i(t_i) - p_{\text{exp}}^r(t_i) \right) = 0 \quad (26)$$

and

$$\sum_{i=1}^{i=N} p^i(t_i) \left(\frac{a-1}{a+1} p^i(t_i) - p_{\text{exp}}^r(t_i) \right) = 0, \quad (27)$$

which is equivalent to

$$a = \frac{\sum_{i=1}^{i=N} p^i(t_i) (p^i(t_i) + p_{\text{exp}}^r(t_i))}{\sum_{i=1}^{i=N} p^i(t_i) (p^i(t_i) - p_{\text{exp}}^r(t_i))} = \frac{\alpha_{\infty} \cos \theta}{\phi \sqrt{\alpha_{\infty} - \sin^2 \theta}}, \quad (28)$$

the expression of the porosity is

$$\phi = \frac{\sum_{i=1}^{i=N} p^i(t_i) (p^i(t_i) - p_{\text{exp}}^r(t_i))}{\sum_{i=1}^{i=N} p^i(t_i) (p^i(t_i) + p_{\text{exp}}^r(t_i))} \left(\frac{\alpha_{\infty} \cos \theta}{\sqrt{\alpha_{\infty} - \sin^2 \theta}} \right). \quad (29)$$

The second derivative term:

$$\begin{aligned} \frac{\partial^2 U}{\partial a^2} = & - \frac{8}{(a+1)^3} \sum_{i=1}^{i=N} \left(\frac{a-1}{a+1} (p^i(t_i))^2 - p_{\text{exp}}^r(t_i) \cdot p^i(t_i) \right) \\ & + \frac{8}{(a+1)^4} \sum_{i=1}^{i=N} (p^i(t_i))^2, \end{aligned} \quad (30)$$

from Eq. (26), we have

$$\frac{\partial^2 U}{\partial a^2} = - \frac{2}{(a+1)} \frac{\partial U}{\partial a} + \frac{8}{(a+1)^4} \sum_{i=1}^{i=N} (p^i(t_i))^2, \quad (31)$$

when $\partial U / \partial a = 0$, the condition $\partial^2 U / \partial a^2 > 0$ is always verified.

Relation (29) is the expression of the porosity as a function of the tortuosity, the incidence angle θ , and the discrete set of values of the incident and reflected signal, we will use this relation in Sec. V to estimate the value of the porosity from experimental incident and reflected data.

V. ULTRASONIC MEASUREMENTS

As an application of this model, some numerical simulations are compared to experimental results. Experiments are carried out in air with two broadband Ultrason NCT202

transducers having a 190 kHz central frequency in air and a bandwidth at 6 dB extending from 150 kHz to 230 kHz. Pulses of 400 V are provided by a 5052PR Panametrics pulser/receiver. The received signals are amplified up to 90 dB and filtered above 1 MHz to avoid high-frequency noise. Electronic perturbations are removed by 1000 acquisition averages. The experimental setup is shown in Fig. 5. The duration of the signal plays an important role, its spectrum must verify the condition of high-frequency approximation referred to in Sec. IV.

Figures 6(a) and 6(b) show the incident and reflected experimental signals, respectively, at the incident angle 17° by the plastic foam M2. The parameters of the plastic foam M2 are: thickness 4.1 cm, resistivity $\sigma = 3000 \text{ Nm}^{-4} \text{ s}$, $\alpha_\infty = 1.07$, $\Lambda = 230 \mu\text{m}$, and $\Lambda' = 690 \mu\text{m}$. Figures 7(a) and 7(b) show the incident and reflected experimental signals, respectively, at the incident angle 53° by the plastic foam M2.

Figures 8(a) and 8(b) show the spectra of the incident and reflected experimental signals, respectively, at the incidence angle 17° . Figures 9(a) and 9(b) show the spectra of the incident and reflected experimental signals, respectively, at the incident angle 53° . From the spectra of the incident and reflected signals, the reader can see that they have the same bandwidths which means that there is no dispersion. This concurs with the theory which predicts that the reflected wave from the first interface $x=0$ is measured and simply attenuated by the factor $(\alpha_\infty \cos \theta - \phi \sqrt{\alpha_\infty - \sin^2 \theta}) / \alpha_\infty \cos \theta + \phi \sqrt{\alpha_\infty - \sin^2 \theta}$.

Using the incident and reflected experimental data for the foam M2 and relation (29), the values of the porosity optimized by solving the inverse problem for each incidence angle are given in Table I. The average value of the porosity obtained is $\phi = 0.97$.

Figures 10 and 11 show the comparison between experimental reflected signals and simulated reflected signals for the optimized value of the porosity ($\phi = 0.97$), the difference between the predicted and experimental curves are slight which leads us to conclude that the optimized value of the porosity is good. The value of the porosity of the foam M2 given by the porosimeter^{10,18} is $\phi = 0.96 \pm 0.02$. The flow resistivity of the plastic foam M2 is $\sigma = 3000 \text{ Nm}^{-4} \text{ s}$. This value is low compared with other plastics foams, and is the reason why the value of the porosity is very close to 1 and thus the reflected signals by the plastic foam M2 is very small near the incident signals.

Another plastic foam M3 is studied (thickness 0.6 cm). This has a high level of flow resistivity, $\sigma = 125000 \text{ Nm}^{-4} \text{ s}$ and the ultrasonic parameters are $\alpha_\infty = 1.7$, $\Lambda = 23 \mu\text{m}$, and $\Lambda' = 69 \mu\text{m}$. Figures 12 and 13 show the incident and reflected signals at the incidence angles 13° and 39° , respectively.

Figures 14 and 15 show their spectra, respectively. Here again, we can conclude from the spectra of the incident and reflected signals that there is no dispersion. By solving the inverse problem from the incident and reflected data and relation (29), the optimized values of the porosity for each incidence angle are given in Table II. The average value of the porosity obtained is $\phi = 0.82$. Figures 16 and 17 show the

comparison between simulated reflected signals obtained by the optimized value of the porosity for each incidence angle and the experimental signals. The readers can see the slight difference between the experimental and simulated signals that proves the optimized value of the porosity. The main advantage of this method is its simplicity compared with the porosimeter,¹⁸ which involves more complicated measurement steps and a more expensive experimental setup.

APPENDIX: GREEN FUNCTION OF THE MEDIUM

The Green function of the propagation [Eq. (6)] is given in Ref. 3 by

$$F(t, k) = \begin{cases} 0 & \text{if } 0 \leq t \leq k \\ \Xi(t) + \Delta \int_0^{t-k} h(t, \xi) d\xi, & \text{if } t \geq k \end{cases},$$

with

$$\Xi(t) = \frac{b'}{4\sqrt{\pi}} \frac{k}{(t-k)^{3/2}} \exp\left(-\frac{b'^2 k^2}{16(t-k)}\right),$$

where $h(\tau, \xi)$ has the following form:

$$h(\xi, \tau) = -\frac{1}{4\pi^{3/2}} \frac{1}{\sqrt{(\tau-\xi)^2 - k^2}} \frac{1}{\xi^{3/2}} \times \int_{-1}^1 \exp\left(-\frac{\chi(\mu, \tau, \xi)}{2}\right) (\chi(\mu, \tau, \xi) - 1) \frac{\mu d\mu}{\sqrt{1-\mu^2}},$$

and where $\chi(\mu, \tau, \xi) = (\Delta \mu \sqrt{(\tau-\xi)^2 - k^2} + b'(\tau-\xi))^2 / 8\xi$, $b' = B c_0^2 \sqrt{\pi}$, $c' = C \cdot c_0^2$, and $\Delta = b'^2 - 4c'$, when $k \rightarrow \infty$, Ξ and $h(\xi, \tau)$ tend toward zero, then the Green function $F(t, k)$ also tends toward zero.

- ¹Z. E. A. Fellah and C. Depollier, J. Acoust. Soc. Am. **107**, 683 (2000).
- ²Z. E. A. Fellah and C. Depollier, J. Comp. Acoust. **9**, 1163 (2001).
- ³Z. E. A. Fellah, C. Depollier, and M. Fellah, J. Sound Vib. **244**, 359 (2001).
- ⁴Z. E. A. Fellah, C. Depollier, and M. Fellah, Acta Acust. (Eur. J.) **88**, 34 (2002).
- ⁵D. L. Johnson, J. Koplik, and R. Dashen, J. Fluid Mech. **176**, 379 (1987).
- ⁶J. F. Allard, *Propagation of Sound in Porous Media: Modeling Sound Absorbing Materials* (Chapman and Hall, London, 1993).
- ⁷M. A. Biot, J. Acoust. Soc. Am. **28**, 168 (1956).
- ⁸M. A. Biot, J. Acoust. Soc. Am. **28**, 179 (1956).
- ⁹K. Attenborough, Phys. Lett. **82**, 179 (1982).
- ¹⁰L. L. Beranek, J. Acoust. Soc. Am. **13**, 248 (1942).
- ¹¹C. Zwikker and C. W. Kosten, *Sound Absorbing Materials* (Elsevier, New York, 1949).
- ¹²Y. Champoux and J. F. Allard, J. Acoust. Soc. Am. **91**, 3346 (1992).
- ¹³D. Lafarge, P. Lemarnier, J. F. Allard, and V. Tarnow, J. Acoust. Soc. Am. **102**, 1995 (1996).
- ¹⁴R. W. Leonard, J. Acoust. Soc. Am. **20**, 39 (1948).
- ¹⁵E. Guyon, L. Oger, and T. J. Plona, J. Phys. D **20**, 1637 (1987).
- ¹⁶D. L. Johnson, T. J. Plona, C. Scala, F. Psierb, and H. Kojima, Phys. Rev. Lett. **49**, 1840 (1982).
- ¹⁷J. Van Brakel, S. Modry, and M. Svata, Powder Technol. **29**, 1 (1981).
- ¹⁸Y. Champoux, M. R. Stinson, and G. A. Daigle, J. Acoust. Soc. Am. **89**, 910 (1991).
- ¹⁹S. G. Samko, A. A. Kilbas, and O. I. Marichev, *Fractional Integrals and Derivatives: Theory and Applications* (Gordon and Breach Science, Amsterdam, 1993).
- ²⁰P. Leclaire, L. Kelders, W. Lauriks, N. R. Brown, M. Melon, and B. Castagnède, J. Appl. Phys. **80**, 2009 (1996).
- ²¹N. Brown, M. Melon, V. Montebault, B. Castagnède, W. Lauriks, and P. Leclaire, C. R. Acad. Sci. Paris **322**, 121 (1996).